Supporting Information for Predicting Polyacrylate-Microplastic Interactions with Atomistic Simulation

Timothy M.E. Jugovic,[a] Henry E. Thurber,[b] Michael T. Robo,[a] Woojung Ji,[a] Madeline Clough,[a] Anne J. McNeil,[a,b] and Paul M. Zimmerman[a]*

a. Department of Chemistry, University of Michigan, 930 North University Avenue, Ann Arbor, Michigan, 48109-1055

b. Macromolecular Science and Engineering Program, University of Michigan, 2800 Plymouth Road, Ann Arbor, Michigan 48109-2800, United States

*paulzim@umich.edu

Table of contents

1. Work of adhesion derivation S2

2. Further microplastic computational details S3

3. Literature and computational values for density of polyacrylate adhesives and microplastic particles S4

4. CHARMM stability analysis S5

5. Representative structures of 50% R* polyacrylate adhesives (in vacuo) S8

6. Simulation determinations of surface energy contributions S9

7. Polyacrylate monomer sequences S10

8. Polarity difference versus aqueous work of adhesion S10

9. Polyacrylate adhesives before and after aqueous simulation S12

10. Hydrogen bond determination method S13

11. Computational surface area data S15

12. Interfacial tension for adhesives with different microplastics S16

13. Additional polystyrene contacts with adhesives S18

14. Inequality relationship for adhesive-microplastic surface tension S22

15. Computational cost analysis S23

16. Experimental procedures S24

17. Experimental tables and figures S26

18. References S32

1. Work of adhesion derivation

Work of adhesion (WoA) is calculated through the following:

$$W_{12}^{Adh} = \gamma_1 + \gamma_2 - \gamma_{12} \quad \text{(S1)}$$

where γ_1, γ_2 is the surface tension (e.g., water's surface tension) and γ_{12} is the interfacial tension between the two surfaces in contact. When three materials may form interfaces with one another,

$$W_{adh-plas(wat)}^{Adh} = W_{adh-plas}^{Adh} - W_{adh-wat}^{Adh} - W_{plas-wat}^{Adh} + W_{wat-wat}^{Adh} \quad \text{(S2)}$$

WoA between an adhesive and plastic increases (predicted to stick together) when $W_{wat-wat}^{Adh}$ grows more positive (meaning the adhesive and plastic are sticky and water doesn't want to form new surfaces) and $W_{adh-wat}^{Adh}$, $W_{plas-wat}^{Adh}$ become more negative (meaning water doesn't want to form interactions with either the adhesive or plastics). The value of $W_{wat-wat}^{Adh}$ is non-zero because of equation (S1):

$$W_{wat-wat}^{Adh} = \gamma_{wat} + \gamma_{wat} - \gamma_{wat-wat} \quad \text{(S3)}$$

and since $\gamma_{wat-wat} = 0$ (as all self-interactions are defined as 0)

$$W_{wat-wat}^{Adh} = 2\gamma_{wat} \quad \text{(S4)}$$

which is defined as the work of cohesion (from the literature):

$$W_{L}^{Coh} = 2\gamma_L \quad \text{(S5).}$$

W_{wat}^{Coh} is preferred over W_{adh}^{Coh} because the adhesive and plastic surfaces are coming together underwater, so they displace the aqueous medium around them and form new interfaces with water, but not new surfaces themselves so their cohesion doesn't affect the overall $W_{adh-plas(wat)}^{Adh}$

Filling in the variables for Equation (S2) using Equation (S1)

$$W_{adh-plas(wat)}^{Adh} = \gamma_{adh} + \gamma_{plas} - \gamma_{adh-plas} - (\gamma_{adh} + \gamma_{wat} - \gamma_{adh-wat}) - (\gamma_{plas} + \gamma_{wat} - \gamma_{plas-wat}) + 2\gamma_{wa} \quad \text{(S6)}$$

This can rearrange to:

$$W_{adh-plas(wat)}^{Adh} = \gamma_{adh} - \gamma_{adh} + \gamma_{plas} - \gamma_{plas} - \gamma_{adh-plas} + \gamma_{adh-wat} + \gamma_{plas-wat} - \gamma_{wat} - \gamma_{wat} + 2\gamma_{wat} \quad \text{(S7)}$$

and then reduce to:

$$W_{adh-plas(wat)}^{Adh} = -\gamma_{adh-plas} + \gamma_{adh-wat} + \gamma_{plas-wat} \quad \text{(S8)}$$

Arriving at the final intended $W_{adh-plas(wat)}^{Adh}$

$$W_{adh-plas(wat)}^{Adh} = \gamma_{adh-wat} + \gamma_{plas-wat} - \gamma_{adh-plas} \quad \text{(S9)}$$

2. Further microplastic computational details

Initial structures of polymers (nylon-6 (PA-6), polystyrene (PS), and high-density polyethylene (HDPE)) were generated with CHARMM-GUI as long linear chains. CHARMM-GUI additionally provided pre-parameterized forcefields for each polymer, which are included in cgenff 4.0. Water was represented by the TIP3P force field.[1] As indicated in the main text, CHARMM was used to relax polymers to idealized densities at room temperature, *in vacuo* into a MP particle. A single chain was generated for each polymer. Nylon-6 (PA-6) was generated as a 200-meric unit chain, PS was generated as a 600-meric unit chain, and HDPE was generated as a 300-meric unit chain. For PA-6 and PS, relaxation occurred as indicated in a 1 ns simulation at 298 K. However, HDPE initially relaxed into a crystal structure that was too low density compared to experimental values. As such the initially relaxed structure was re-simulated at an initial 400K for 0.5 ns, before the simulation temperature was reduced from 400K to 298K over an additional 0.5 ns. As HDPE density agreed with literature values after the secondary simulation, this new structure was used for subsequent modeling. Periodic boundary conditions were used for all MD simulations.

For polyethylene terephthalate (PETE), an initial 4-mer structure was generated using Avogadro, which was parameterized using the Match program, which provides parameterization for identifiable monomers within cgenff. Using the initial parameters provided by Match and present in cgenff 4.0, a longer 128-meric chain of PETE was relaxed into a crystal structure using the same 1 ns, 298 K and *in vacuo* conditions. This relaxed crystal structure was then copied 3 times to produce a 384-unit surface in three separate crystal blocks, which was again simulated at 1 ns, 298 K and *in vacuo* conditions. The final structure was found to have a density consistent with experimental values and used for subsequent modeling.

Packmol[2] was used to surround the substrates with water in the aqueous phase microplastics/adhesives simulations. The water box was equilibrated for 25 ns under NPT conditions to condense the water down to standard pressure, then ran at 5 ns at NVT for calculating interfacial energies.

Over the timescale of the equilibrium trajectories, we observed nontrivial surface interactions between polyacrylate with poly(tridecafluorooctyl acrylate) (TDO) sidechains and PS being formed and removed as the system was sampled. This indicates that sufficient timescales were propagated to allow the system to reach their preferred configurations.

The contact surface area is computed using standard CHARMM methodology for solvent-accessible surface area (SASA). First, the SASA of each unit ($A_{plastic}$, $A_{adhesive}$) is computed using the "coor surf" keyword, then the SASA is determined for the combination of the two types ($A_{plastic + adhesive}$). The former was subtracted from the latter to give the contact area ($A_{contact}$), shown in Equation S10. The probe radius for SASA calculations was set at 1.4 Å.

$$A_{contact} = -(A_{plastic + adhesive} - A_{plastic} - A_{adhesive}) \quad \text{(S10)}$$

3. Literature and computational values for density of polyacrylate adhesives and microplastic particles

Table S1. Comparison of experimental and computational density values for microplastics and adhesives

polymer	comp. mass (Da)	comp. volume (Å^3)	comp. ρ (g/cm^3)	exp. ρ (g/cm^3)[3]
PS	62400	102700 ± 260	1.01 ± 0.01	1.00 ± 0.05
PA-6	22600	33390 ± 90	1.13 ± 0.01	1.14 ± 0.02
HDPE	8420	14210 ± 70	0.98 ± 0.01	0.96 ± 0.02
PETE	67600	80820 ± 40	1.39 ± 0.01	1.41 ± 0.05
teflon	N/A	N/A	N/A	2.2 ± 0.00
poly(2-ethylhexyl acrylate) (2-EH)	36900	59400 ± 120	1.03 ± 0.01	0.96 ± 0.07
poly(benzyl acrylate) (ben)	N/A	N/A	N/A	1.19 ± 0.02
50% ben	43800	68500 ± 180	1.06 ± 0.01	N/A
50% poly(3-pyridyl acrylate) (3-pyr)	38900	59700 ± 150	1.08 ± 0.02	N/A
50% poly(2-tetrahydrofurfuryl acrylate) (THF)	36000	60600 ± 260	0.99 ± 0.01	N/A
50% TDO	38000	41600 ± 170	1.52 ± 0.01	N/A

Table S2. Comparison of experimental and computational interaction energies for microplastics and adhesives

θ_{SL} is contact angle for water, γ_{SL} (surface-liquid) is the interaction energy between surface and water, γ_{SG} (surface-gas) is the interaction energy of the surface with air.

polymer	θ_{SL}	γ_{SG} (mN/m)	exp. γ_{SL} (mN/m)	comp. γ_{SL} (mN/m)
PS[48]	87.4	34	30.7 ± 2.4	32.4 ± 0.2
PA-6[49]	68.3	42.2	15.6 ± 2.6	12.0 ± 0.2
HDPE[50]	88.4	25.9	23.9 ± 3.2	22.4 ± 0.2
PETE[50]	72.5	43.5	21.8 ± 2.1	19.7 ± 0.1
2-EH	98 ± 1	33.1 ± 1.5	43.1 ± 2.7	49.1 ± 0.5
50% ben	96 ± 2	33.6 ± 2.0	41.1 ± 2.4	53.9 ± 0.7

4. CHARMM stability analysis

The following plots show the sampled interaction energies and areas for poly(2-ethylhexyl acrylate) (2-EH) after a 25 ns equilibration and then over the course of a 5 ns simulation. They indicate consistent sampling of the ratio of energy to surface area, based on maintenance of surface-to-surface contact during the MD.

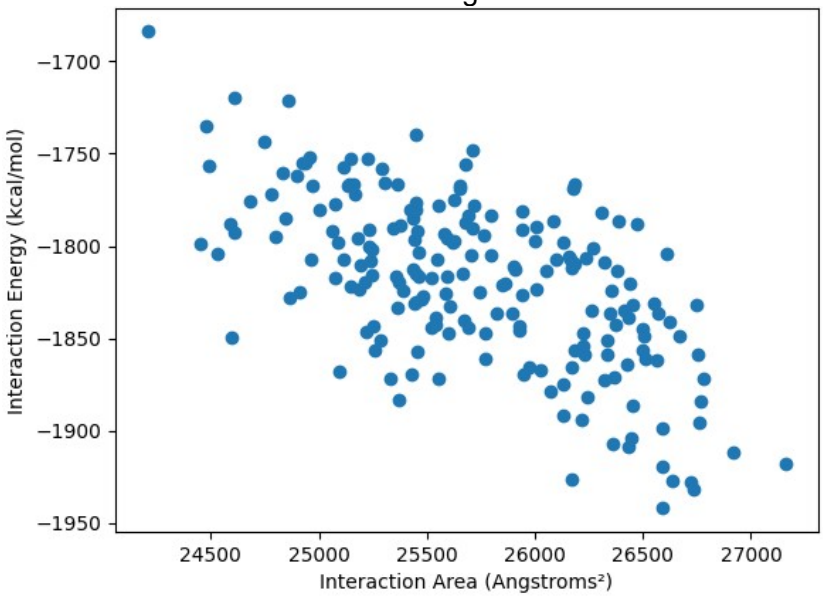

Figure S1. Interaction energy versus interaction area for 2-EH with water molecules for 25 ps snapshots from simulation of 5 ns.

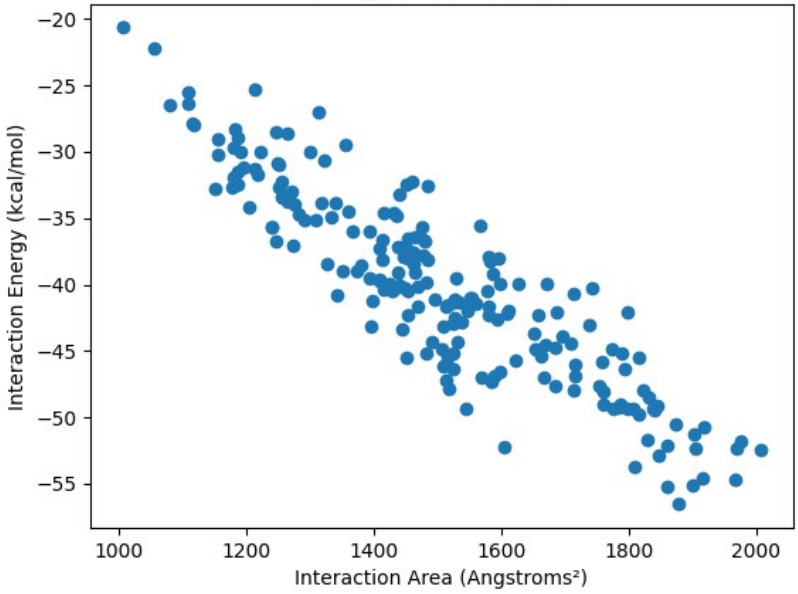

Figure S2. Interaction energy versus interaction area for 2-EH with HDPE surface for 25 ps snapshots from simulation of 5 ns.

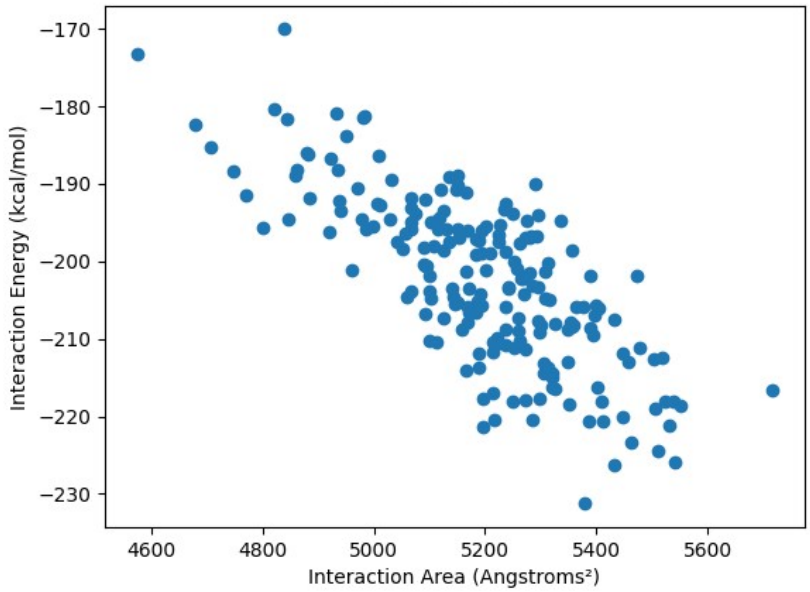

Figure S3. Interaction energy versus interaction area for 2-EH with PETE surface for 25 ps snapshots from simulation of 5 ns.

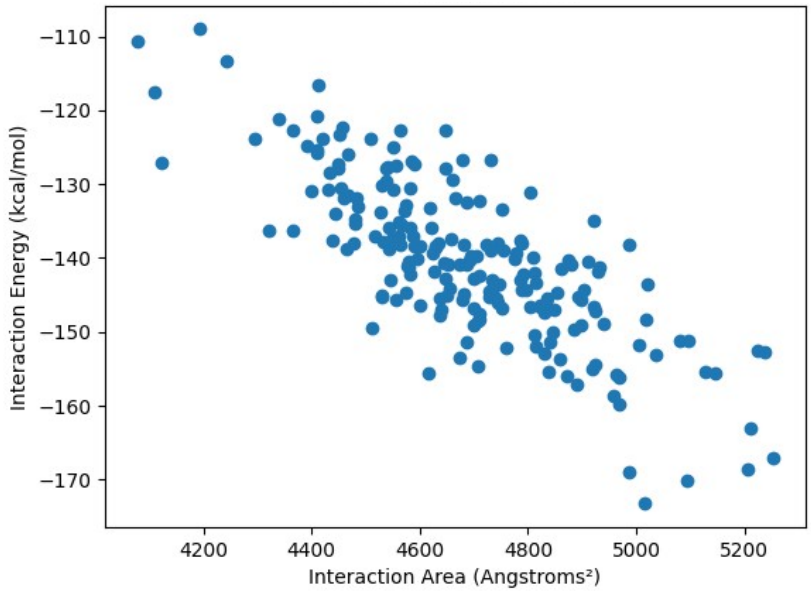

Figure S4. Interaction energy versus interaction area for 2-EH with PS surface for 25 ps snapshots from simulation of 5 ns.

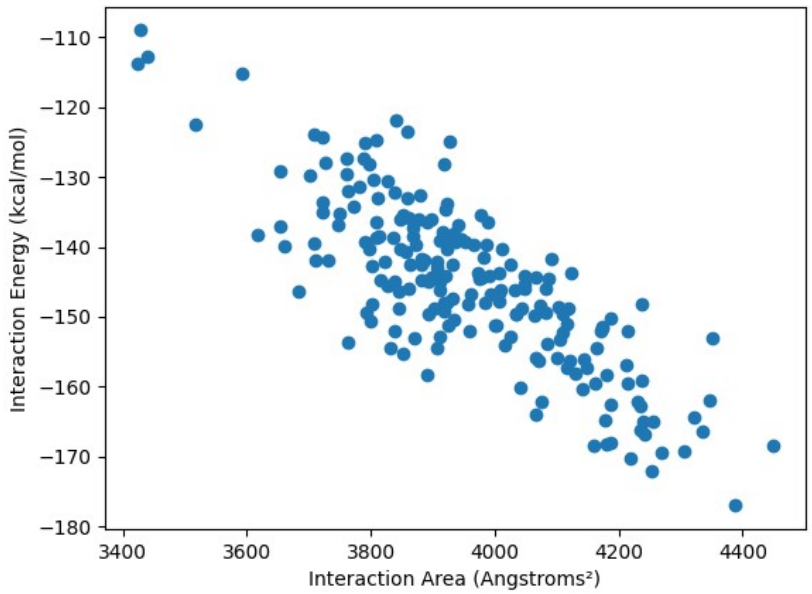

Figure S5. Interaction energy versus interaction area for 2-EH with PA-6 surface for 25 ps snapshots from simulation of 5 ns.

5. Representative structures of 50% R* polyacrylate adhesives (in vacuo)

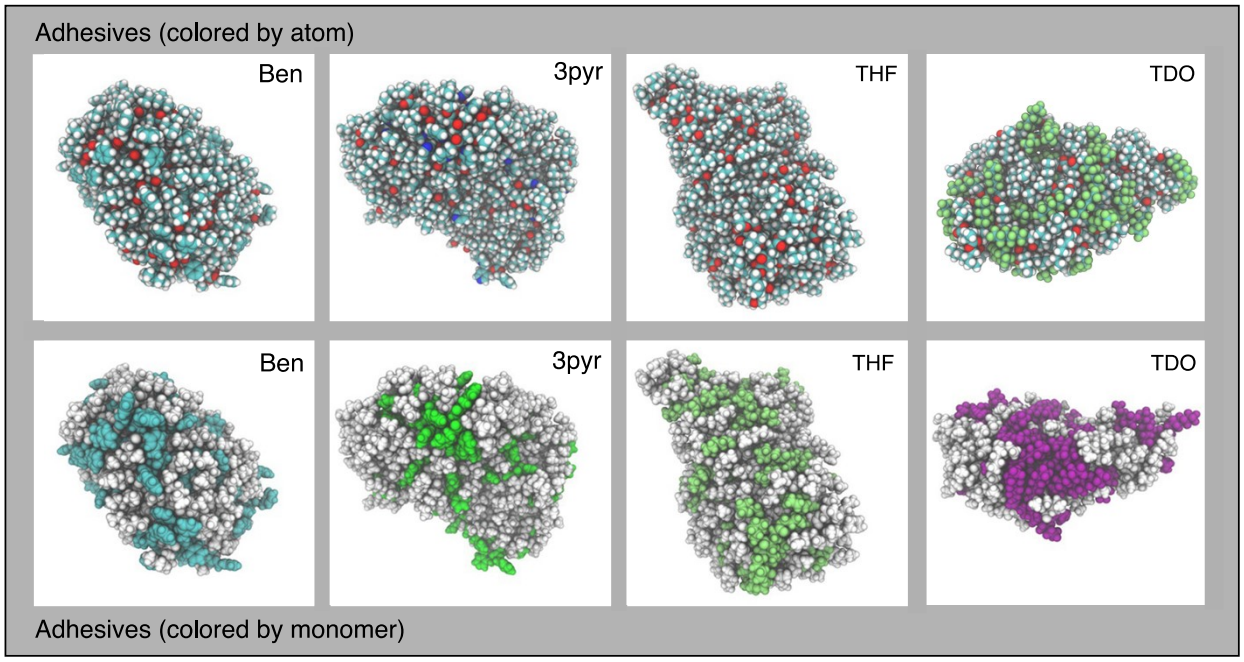

adhesive	surface area (Å^2)	volume (Å^3)	SA:V (Å^{-1})	density (g/cm^3)
50% THF (vacuo)	18380 ± 30	60600 ± 260	0.30 ± 0.02	0.810 ± 0.003
50% THF (aqueous)	23300 ± 170	60000 ± 600	0.39 ± 0.03	0.814 ± 0.008
50% TDO (vacuo)	14100 ± 30	41600 ± 170	0.34 ± 0.01	1.101 ± 0.004
50% TDO (aqueous)	16200 ± 270	41700 ± 400	0.39 ± 0.05	1.100 ± 0.01

Figure S6. Top: Polyacrylate adhesives in vacuo at 50% R incorporation, left to right, ben, 3-pyr, THF, TDO. Atom legend (top): C (light blue), O (red), H (white), N (dark blue), and F (light green). Residue legend (bottom): 2-EH (white), ben (blue), 3-pyr (bright green), THF (dull green), and TDO (purple). Averages were determined by periodic sampling of MD simulations with error from standard deviation. Bottom: Table of vacuo vs. aqueous changes in surface area, volume, SA:V ratio, and density for 50%THF and 50% TDO adhesives.

6. Simulation determinations of surface energy contributions

Table S3. Computational work of adhesion and surface energy contributions for 100% 2-EH with four different plastic identities.

100% 2-EH	$W^{Adh}_{adh-plas(wat)}$ (mN/m)	$\gamma_{adh-wat}$ (mN/m)	$\gamma_{plas-wat}$ (mN/m)	$\gamma_{adh-plas}$ (mN/m)
PETE	43.25	-49.12	-19.73	-25.60
PS	62.18	-49.12	-32.37	-19.31
HDPE	52.83	-49.12	-22.46	-18.75
PA-6	36.6	-49.12	-12.00	-24.52

Table S4. Computational work of adhesion and surface energy contributions for 50% ben with four different plastic identities.

50% ben	$W^{Adh}_{adh-plas(wat)}$ (mN/m)	$\gamma_{adh-wat}$ (mN/m)	$\gamma_{plas-wat}$ (mN/m)	$\gamma_{adh-plas}$ (mN/m)
PETE	47.07	-53.91	-19.73	-26.57
PS	65.17	-53.91	-32.37	-21.11
HDPE	55.8	-53.91	-22.46	-20.57
PA-6	39.51	-53.91	-12.00	-26.40

Table S5. Computational work of adhesion and surface energy contributions for 50% 3-pyr with four different plastic identities.

50% 3-pyr	$W^{Adh}_{adh-plas(wat)}$ (mN/m)	$\gamma_{adh-wat}$ (mN/m)	$\gamma_{plas-wat}$ (mN/m)	$\gamma_{adh-plas}$ (mN/m)
PETE	51.35	-58.93	-19.73	-27.31
PS	71.28	-58.93	-32.37	-20.02
HDPE	60.3	-58.93	-22.46	-21.09
PA-6	41.48	-58.93	-12.00	-29.45

Table S6. Computational work of adhesion and surface energy contributions for 50% THF with four different plastic identities.

50% THF	$W^{Adh}_{adh-plas(wat)}$ (mN/m)	$\gamma_{adh-wat}$ (mN/m)	$\gamma_{plas-wat}$ (mN/m)	$\gamma_{adh-plas}$ (mN/m)
PETE	61.45	-69.35	-19.73	-27.63
PS	81.79	-69.35	-32.37	-19.93
HDPE	69.28	-69.35	-22.46	-22.53
PA-6	49.68	-69.35	-12.00	-31.67

Table S7. Computational work of adhesion and surface energy contributions for 50% TDO with four different plastic identities.

50% TDO	$W^{Adh}_{adh-plas(wat)}$ (mN/m)	$\gamma_{adh-wat}$ (mN/m)	$\gamma_{plas-wat}$ (mN/m)	$\gamma_{adh-plas}$ (mN/m)
PETE	40.48	-45.94	-19.73	-25.19
PS	59.46	-45.94	-32.37	-18.85
HDPE	45	-45.94	-22.46	-23.40
PA-6	31.41	-45.94	-12.00	-26.53

7. Polyacrylate monomer sequences

The sequences can be found in separate document or at https://github.com/Shadoon4/polymeriZe/

8. Polarity difference versus aqueous work of adhesion

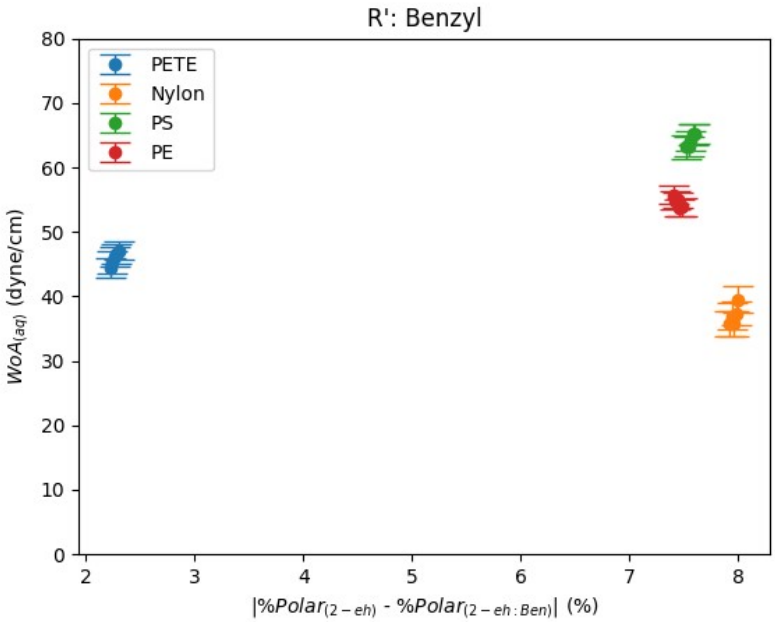

Figure S6. Absolute %polarity difference versus WoA(aq) for ben with 10–50% comonomer incorporation.

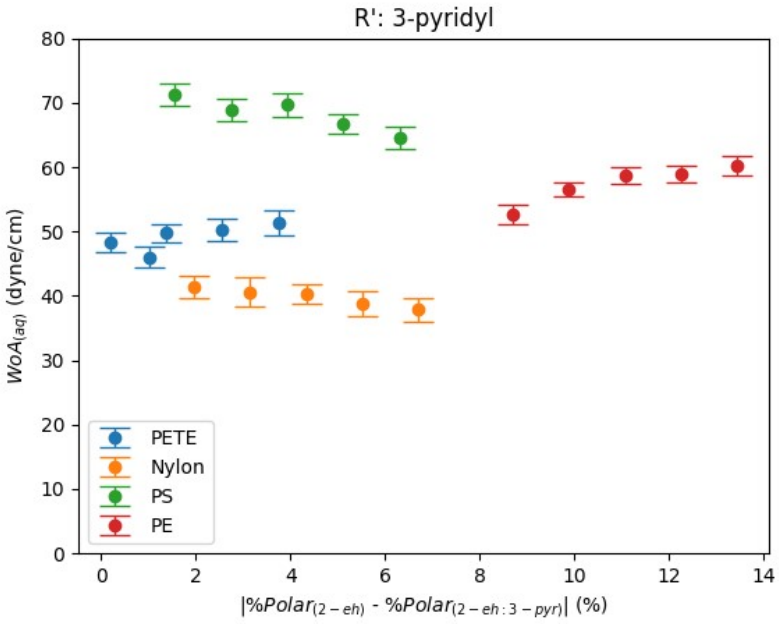

Figure S7. Absolute %polarity difference versus WoA(aq) for 3-pyr with 10–50% comonomer incorporation.

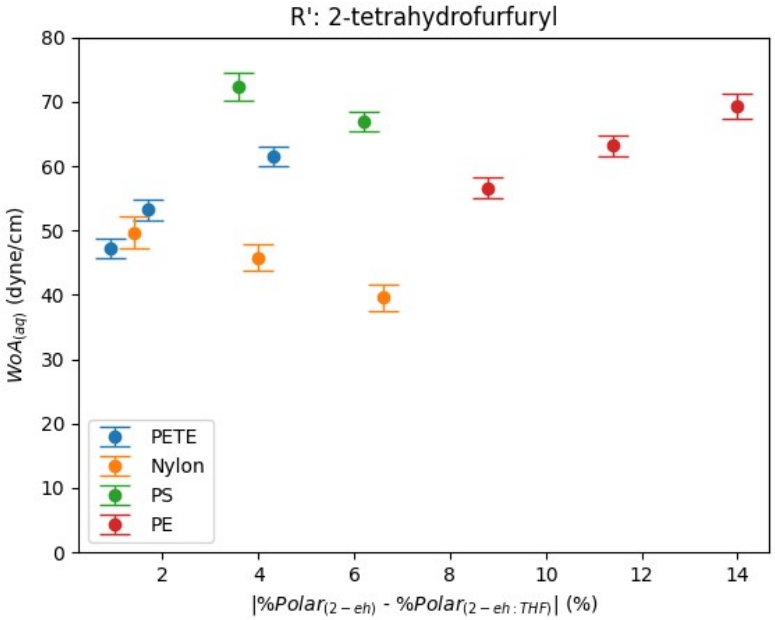

Figure S8. Absolute %polarity difference versus WoA(aq) for THF with 10–50% co-monomer incorporation.

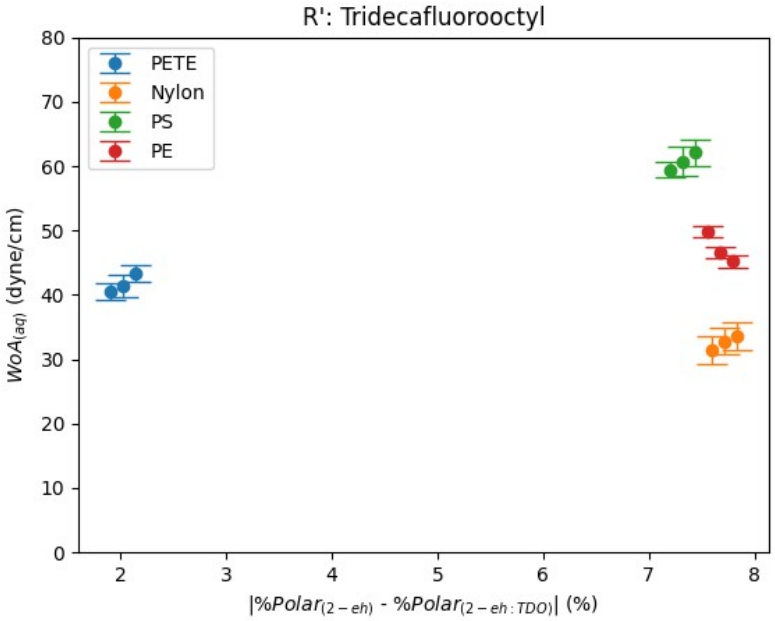

Figure S9. Absolute %polarity difference versus WoA(aq) for TDO with 10–50% co-monomer incorporation.

9. Polyacrylate adhesives before and after aqueous simulation

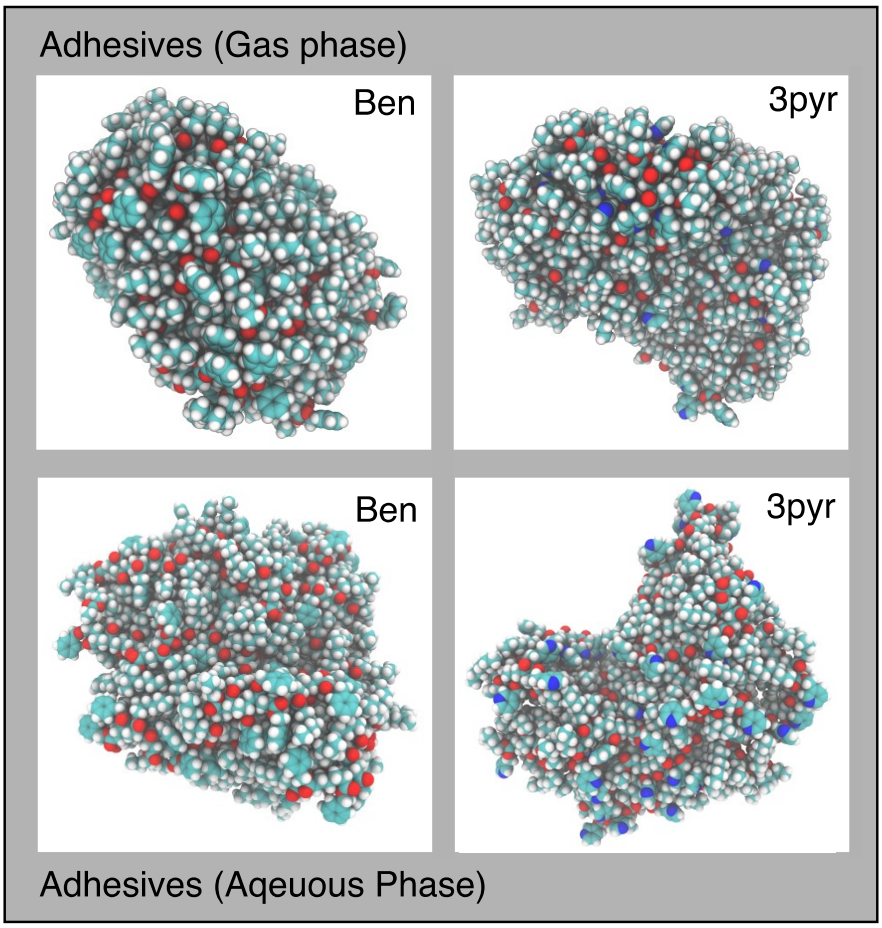

Figure S10. Aqueous rearrangement for representative structures of 50% ben and 50% 3-pyr.

10. Hydrogen bond determination method

H-bonds were assigned using the Visual Molecular Dynamics (VMD) program's built-in H-bond plugin, which determines whether an H-bond is present between atoms in a given selection through the following algorithm:

```
For selection (Donor, Acceptor, Hydrogen) {
        If (Donor-Acceptor distance <= X  && |Donor-Hydrogen-Acceptor Angle| <= Y) {
                H-bond = true
        }
        Else {
                H-bond = false
        }
}
```

Where selections of atoms, *X* distance and *Y* angle are user inputs. H-bond atom selections included the side chains of interest (THF and 3pyr) and water molecules. This selection avoids counting backbone H-bonds as well as H-bonds between water molecules. The distance and angle criteria were set to 3.0 Å and 20°, respectively as these are moderate values for H-bonds [4].

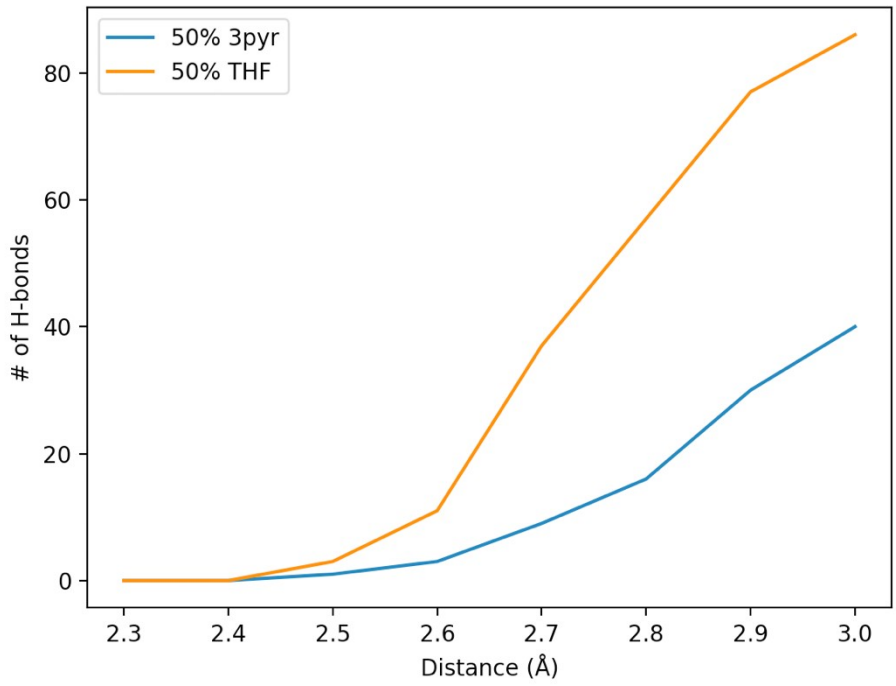

Figure S11. Aggregated H-bond data versus the donor-acceptor distance.

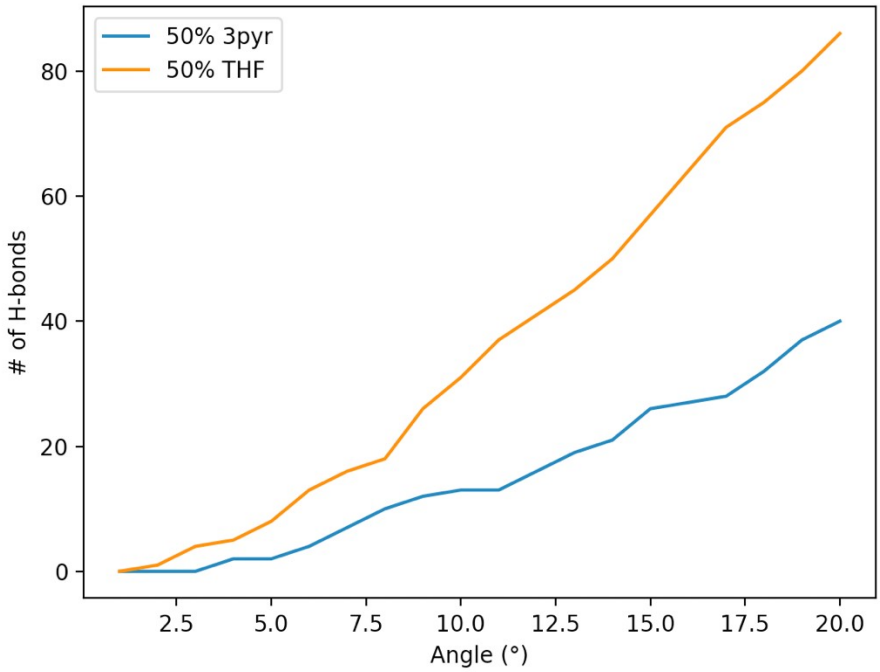

Figure S12. Aggregated H-bond data versus the donor-hydrogen-acceptor angle.

11. Computational surface area data

Table S8. Computational surface area of 50% R* polyacrylates under vacuo and aqueous conditions.

adhesive	surface area vacuo (Å^2)	surface area aqueous (Å^2)
50% ben	18740 ± 30	23200 ± 150
50% 3-pyr	18000 ± 30	19150 ± 80
50% THF	18380 ± 30	23300 ± 170
50% TDO	14100 ± 30	16200 ± 270

12. Interfacial tension for adhesives with different microplastics

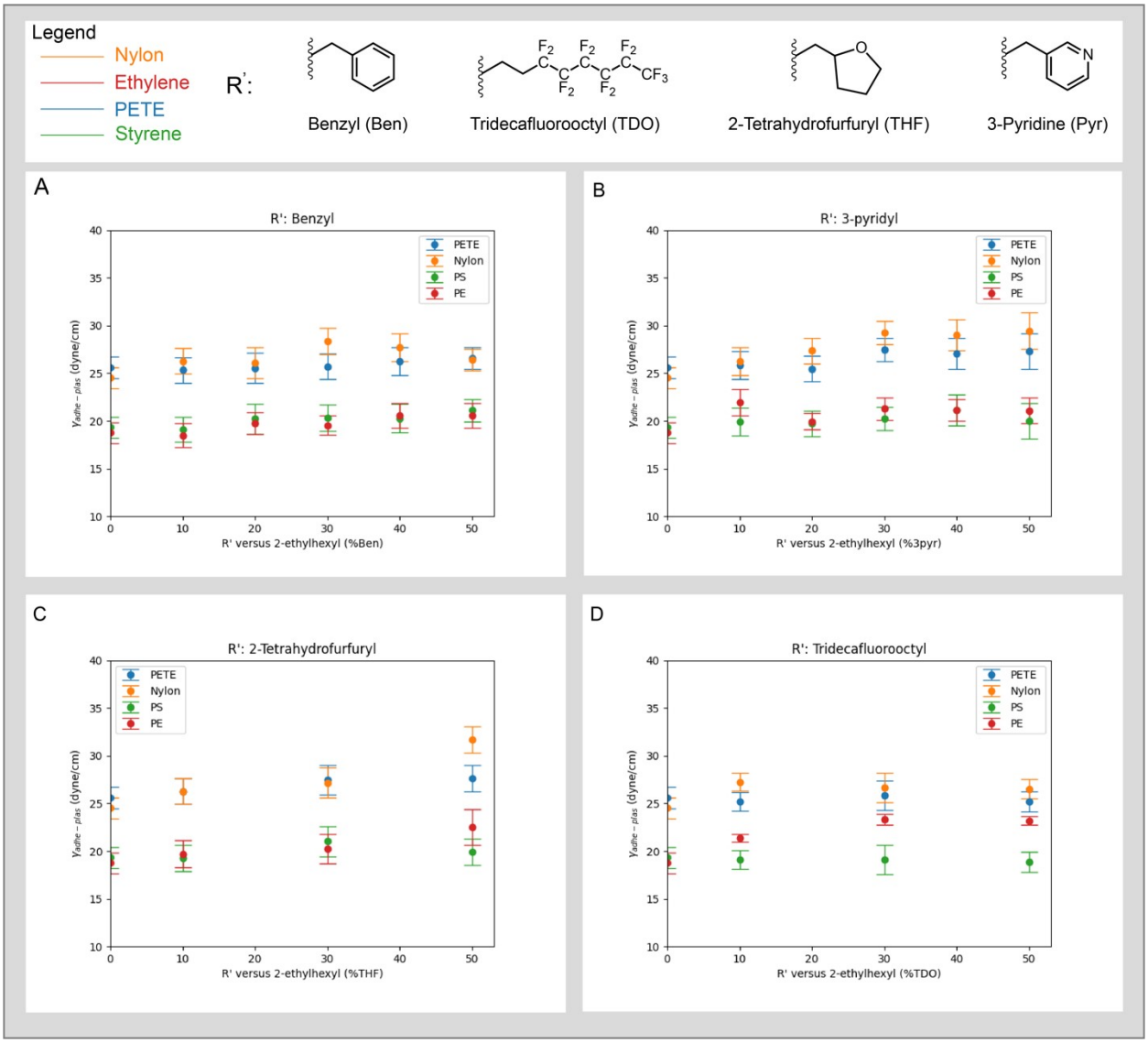

Figure S13. $\gamma_{adh-plas}$ results versus side chain composition for each microplastic and adhesive: (A) ben, (B) 3-pyr, (C) THF, (D) TDO.

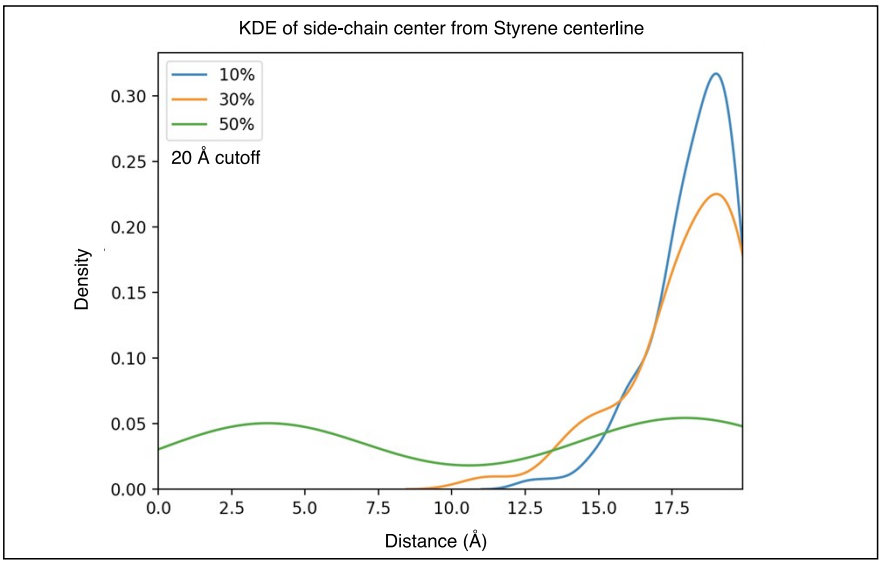

Figure S14. Kernel density estimate (KDE) plot of adhesive side chain center distance from PS centerline for each ratio of %TDO.

13. Additional polystyrene contacts with adhesives

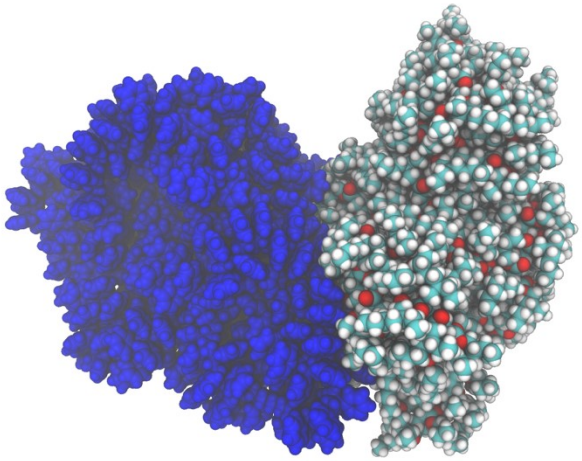

Figure S15. Contact between 100% 2-EH (colored by atom) and PS (blue).

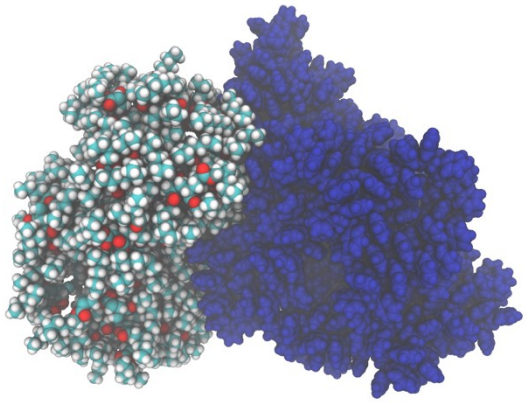

Figure S16. Contact between 10% ben (colored by atom) and PS (blue).

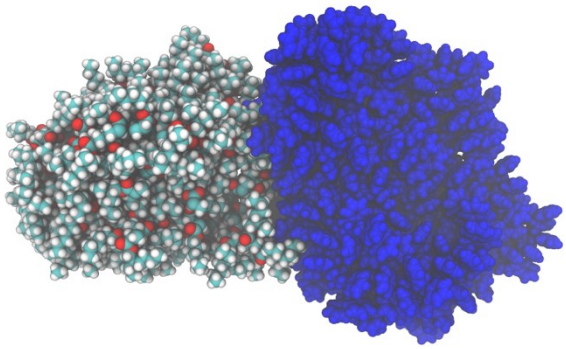

Figure S17. Contact between 30% ben (colored by atom) and PS (blue).

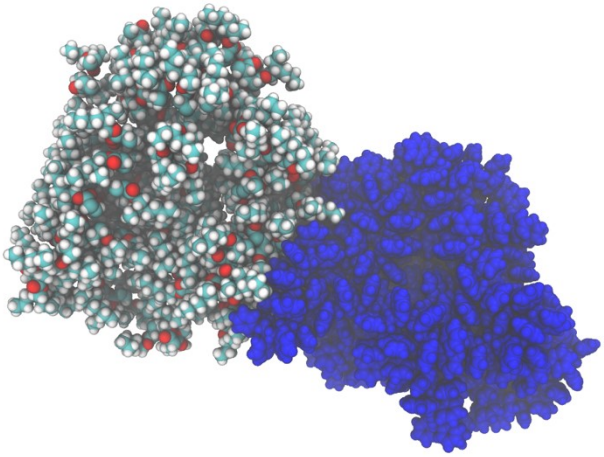

Figure S18. Contact between 50% ben (colored by atom) and PS (blue).

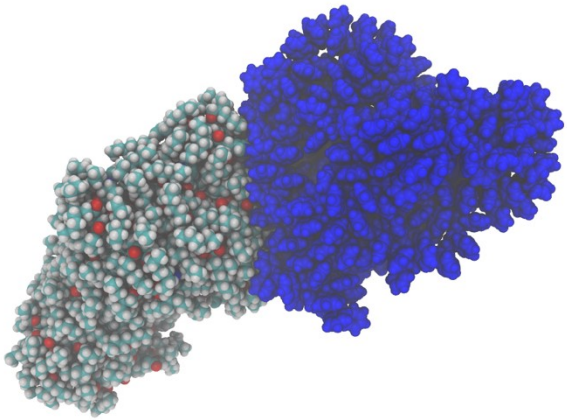

Figure S19. Contact between 10% 3pyr (colored by atom) and PS (blue).

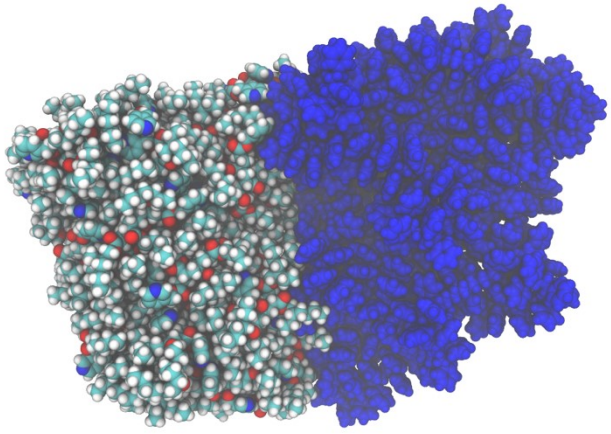

Figure S20. Contact between 30% 3-pyr (colored by atom) and PS (blue).

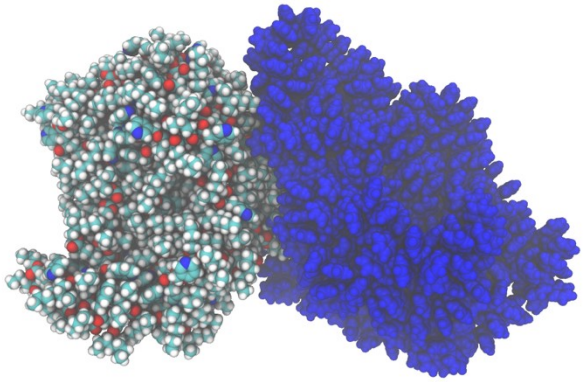

Figure S21. Contact between 50% 3-pyr (colored by atom) and PS (blue).

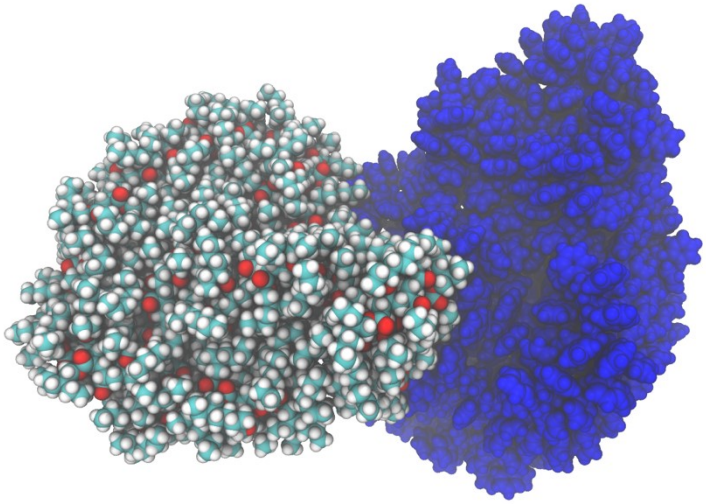

Figure S22. Contact between 10% THF (colored by atom) and PS (blue).

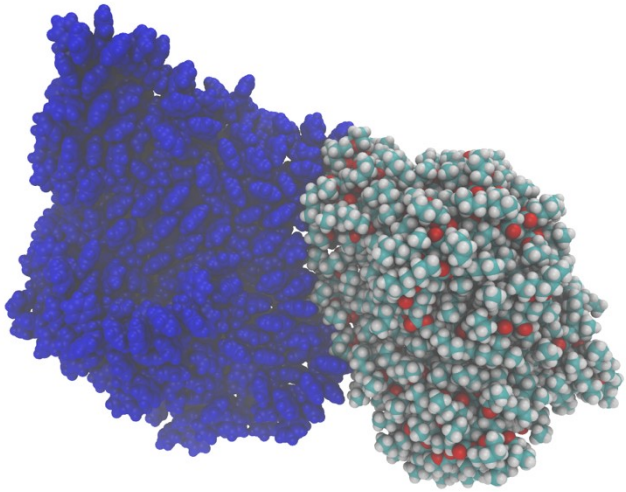

Figure S23. Contact between 30% THF (colored by atom) and PS (blue).

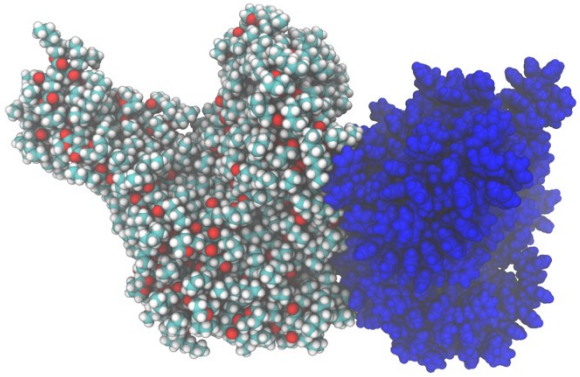

Figure S24. Contact between 50% THF (colored by atom) and PS (blue).

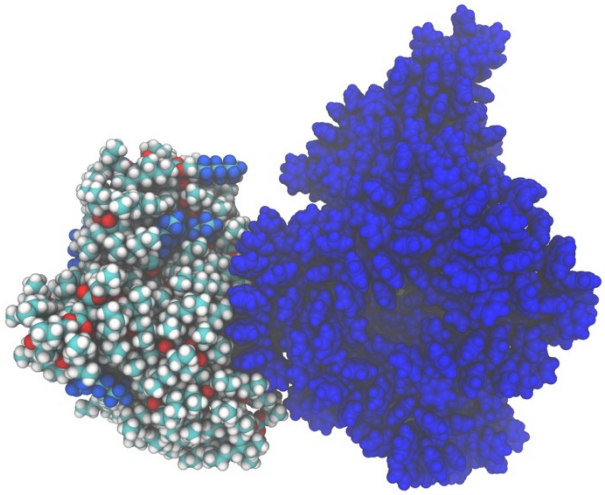

Figure S25. Contact between 10% TDO (colored by atom) and PS (blue).

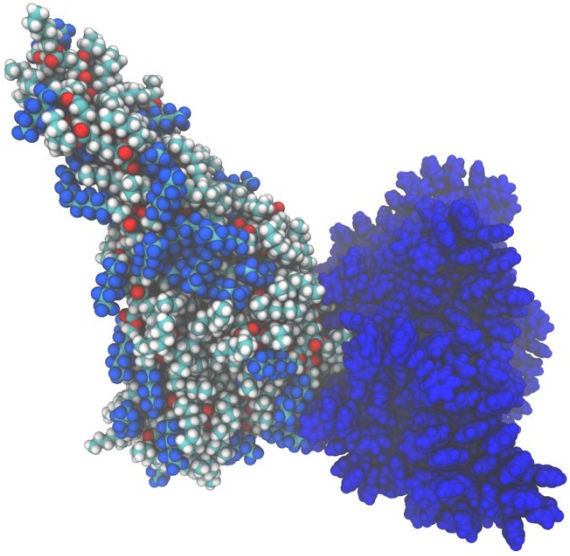

Figure S26. Contact between 30% TDO (colored by atom) and PS (blue).

14. Inequality relationship for adhesive-microplastic surface tension

Equation 1 quantifies the strength of adhesion between surfaces as a function of their individual surface tensions and their interfacial surface tension between them. For any adhesion to occur, the combined surface tension of the two must be more than their interfacial tension, which results in a positive work of adhesion (equation S10).

$$\gamma_{adh-plas} < (\gamma_{plas} + \gamma_{adh}) \quad \text{(S10)}$$

However, the special case of equation 1 is when the interfacial tension is less than each surface tension individually, and not just their combined value (equation S11, S12).

$$\gamma_{adh-plas} < \gamma_{adh} \quad \text{(S11)}$$

$$\gamma_{adh-plas} < \gamma_{plas} \quad \text{(S12)}$$

In that case not only does the whole combined system benefit from forming an interface, but each individual component also benefits from forming an interface over maintaining its individual surface. As a result, the forces that hold the surface together for both components are weaker than those between the two components. Macroscopically, we observe that as the system approaches this state, contact between the components goes from flat to entangled. This results from the interfacial area being energetically favorable to increase and flat interfaces are the minima of contact area.

15. Computational cost analysis

Table S9. Computational time for representative systems and average cost for simulation across all simulations.

system size (#atoms)	25 ns simulation time (hrs)	5 ns simulation time (hrs)
21391	22.79	4.66
20401	22.45	4.51
average simulation time (all simulations):	0.157±0.022	(sec/(atom*ns simulation))

16. Experimental procedures

NMR Spectroscopy – ^{1}H NMR spectra for all polymers were acquired at room temperature on a Varian MR400 spectrometer with a Varian 5 mm PFG AutoX Indirect Detection probe. Chemical shift data are reported in units of δ (ppm) relative to tetramethylsilane (TMS) and referenced with residual solvent. For all ^{1}H NMR spectra, a 3.5 s acquisition time was used with a 10 s relaxation delay between each pulse.

Fourier-Transform Infrared (FTIR) Spectroscopy – FTIR spectroscopy data were obtained on a Thermo-Nicolet IS-50 using the attenuated total reflectance (ATR) accessory on neat polymer samples.

Size Exclusion Chromatography (SEC) – The polymers were dissolved in THF (~1 mg/mL) with mild heating and filtered through a PTFE filter (0.45 μm) into an SEC vial. Polymer molar mass (*M*) and dispersity (Đ) were determined at 40 °C in THF on a SEC: Malvern Viscotek GPCMax VE2001 equipped with two Viscotek LT-5000L 8 mm (ID) × 300 mm S4 (L) columns, and Viscotek TDA 305 and Viscotek RI detectors. Apparent molar masses were calculated using an EasyCal PS-2 standard ranging from 555 to 348,500 g/mol M_n.

Contact Angle Measurements – The surface contact angles of each PSA film were measured for DI water and diiodomethane (>99.0; Aldrich) using an optical goniometer (Ramé-Hart Model 200 (p/n 200-U1)). Polymer films (10 wt% in THF) were deposited on a glass slide via Doctor Blade; their approximate thickness is 42 ± 3 μm, determined from SEM cross-section analysis. The surface contact angles were averaged from four droplets per film and at least three films. The surface energies were calculated using the Owens–Wendt (OW) Method.[5, 6]

Surface Energy Calculation – The surface energy, reported in Table S1, is calculated from the contact angles (measured in air) using equations S13–S14:

$$\left\{(1+cos\theta)\gamma_{LV} = 2\sqrt{\gamma_S^D\gamma_L^D} + 2\sqrt{\gamma_S^P\gamma_L^P}\right\} (S13)$$

$$\gamma_S = \gamma_S^D + \gamma_S^D (S14)$$

where θ is the contact angle of the probe liquid (water or diiodomethane) on the adhesive surface, γ_{LV} is the surface tension of the probe liquid in air, γ_S is the surface tension of adhesive, γ^D and γ^P are the dispersive and polar components of the adhesive surface tensions, respectively.

Probe Tack Measurements – Tack test was conducted using a texture analyzer (Micro Stable Systems, TA×XT-PLUS) with a polished polystyrene, polyethylene terephthalate, high-density polyethylene, and nylon cylinder probe with a diameter of 6 mm. To make the probes, polymer rods were purchased from Goodfellow and cut into a cylindrical shape by the machine shop. The measurements were carried out under DI water on Doctor Bladed adhesive films (10 wt% in THF, thickness; 42 ± 3 μm, determined from SEM cross-section analysis) at a separation rate of 1 cm/s under a constant pressure of 78 mN and a dwell time of 1 s at room temperature. Work of adhesion values were calculated from integrating the area under a force-distance curve.

Synthesis of 2-EH – To a 40 mL vial, PAA (polyacrylic acid; from Sigma Aldrich with reported M_v ~450,000; 600 mg, 8.40 mmol, 1.00 equiv), 2-ethyl hexanol (from Sigma Aldrich with >99.6% purity; 6.53 mL, 41.7 mmol, 5.00 equiv) and H_2SO_4 (0.112 mL, 2.09 mmol, 0.25 equiv) were

added. The vial was then capped and the solution stirred at 120 °C for 10 h. The polymer was purified by dissolving the reaction mixture in minimal amounts of THF (5 mL), precipitating it into MeOH (20 mL), centrifuging and decanting the supernatant. The entire dissolution-precipitation process was repeated five times. The resulting colorless, tacky solid was dried under high vacuum at 80 °C for 10 h. The isolated yield was 64%. See below for ^{1}H NMR spectra and SEC data (M_w = 1,130,000 g/mol; Đ = 3.4).

Synthesis of 42%-ben – To a 40 mL vial, PAA (polyacrylic acid; from Sigma Aldrich with average M_v ~450,000; 600 mg, 8.40 mmol, 1.00 equiv), benzyl alcohol (from Sigma Aldrich with ≥99.9% purity; 2.16 mL, 20.9 mmol, 2.50 equiv), 2-ethyl hexanol (from Sigma Aldrich with >99.6% purity; 3.26 mL, 20.9 mmol, 2.50 equiv) and H_2SO_4 (0.112 mL, 2.09 mmol, 0.25 equiv) were added. The vial was then capped and the solution stirred at 120 °C for 10 h. The polymer was purified by dissolving the reaction mixture in minimal amounts of THF (5 mL), precipitating it into MeOH (20 mL), centrifuging and decanting the supernatant. This entire dissolution-precipitation process was repeated five times. The resulting light brown, tacky solid was dried under high vacuum at 80 °C for 10 h. The isolated yield was 44% and the ratio of side chain incorporation for 2-EH:ben was 58:42. See below for ^{1}H NMR spectra and SEC data (M_w = 1,140,000 g/mol; Đ = 8.5).

17. Experimental tables and figures

Table S10. Water and diiodomethane contact angles of acrylic polymers (2-EH and 42-ben).

sample	water contact angle	sample	diiodomethane contact angle
2-EH Film1 1	96	2-EH Film1 1	50
2-EH Film1 2	97	2-EH Film1 2	49
2-EH Film1 3	99	2-EH Film1 3	50
2-EH Film2 1	96	2-EH Film2 1	54
2-EH Film2 2	98	2-EH Film2 2	54
2-EH Film2 3	97	2-EH Film2 3	54
2-EH Film3 1	97	2-EH Film3 1	53
2-EH Film3 2	98	2-EH Film3 2	56
2-EH Film3 3	99	2-EH Film3 3	51
2-EH Film4 1	98	2-EH Film3 4	52
2-EH Film4 2	97	2-EH Film4 1	52
2-EH Film4 3	101	2-EH Film4 2	50
42-ben Film1 1	95	2-EH Film4 3	51
42-ben Film1 2	96	2-EH Film4 4	55
42-ben Film1 3	96	42-ben Film1 1	50
42-ben Film2 1	96	42-ben Film1 2	50
42-ben Film2 2	95	42-ben Film1 3	50
42-ben Film2 3	95	42-ben Film2 1	51
42-ben Film3 1	95	42-ben Film2 2	51
42-ben Film3 2	95	42-ben Film2 3	52
42-ben Film3 3	97	42-ben Film2 4	52
42-ben Film3 4	97	42-ben Film3 1	49
42-ben Film4 1	96	42-ben Film3 2	51
42-ben Film4 2	97	42-ben Film3 3	52
42-ben Film4 3	95	42-ben Film3 4	51
		42-ben Film4 1	52
		42-ben Film4 2	52
		42-ben Film4 3	50

Table S11. Average and standard deviations of acrylic polymer contact angles determined from the raw data table above.

	water	diiodomethane
2-EH	98 ± 1°	53 ± 2°
42-ben	96 ± 1°	51 ± 1°

Table S12. Calculated surface energies of acrylic polymers from contact angle measurements using equations S13–14.

	dispersive	polar	total	%polarity
2-EH	32.7	0.4	33.1	1
42-ben	32.9	0.7	33.6	2

Table S13. Weight average molar mass and dispersity of acrylic polymers determined from size exclusion chromatography using polystyrene standards.

	M_w (g/mol)	dispersity
2-EH	1,130,000	3.4
42-ben	1,140,000	8.5

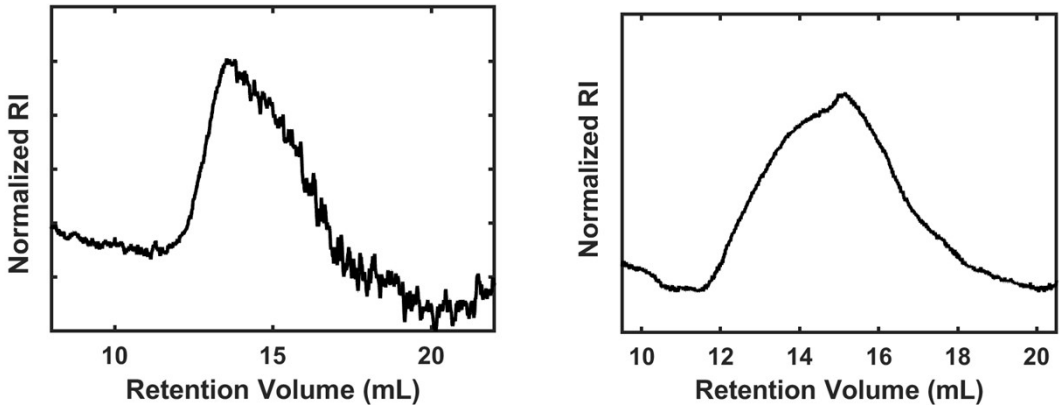

Figure S27. Size-exclusion chromatography traces of 2-EH (left) and 42-ben (right).

Table S14. Experimental work of adhesion determined from probe tack measurements for PS and HDPE probes.

sample	probe	work of adhesion (mJ)	sample	probe	work of adhesion (mJ)
2-EH Film1 1	PS	0.58	2-EH Film1 1	HDPE	0.6
2-EH Film1 2	PS	0.99	2-EH Film1 2	HDPE	0.73
2-EH Film1 3	PS	1.4	2-EH Film1 3	HDPE	0.85
2-EH Film2 1	PS	1.1	2-EH Film2 1	HDPE	0.74
2-EH Film2 2	PS	0.75	2-EH Film2 2	HDPE	0.89
2-EH Film2 3	PS	0.97	2-EH Film2 3	HDPE	0.76
2-EH Film3 1	PS	0.85	2-EH Film3 1	HDPE	0.85
2-EH Film3 2	PS	0.62	2-EH Film3 2	HDPE	0.78
2-EH Film3 3	PS	0.95	2-EH Film3 3	HDPE	0.74
average	PS	0.91	average	HDPE	0.77
standard deviation	PS	0.25	standard deviation	HDPE	0.09
42-ben Film1 1	PS	0.97	42-ben Film1 1	HDPE	0.95
42-ben Film1 2	PS	0.75	42-ben Film1 2	HDPE	1.5
42-ben Film1 3	PS	0.82	42-ben Film1 3	HDPE	0.54
42-ben Film2 1	PS	1.1	42-ben Film2 1	HDPE	0.6
42-ben Film2 2	PS	0.89	42-ben Film2 2	HDPE	0.95
42-ben Film2 3	PS	0.72	42-ben Film2 3	HDPE	0.94
42-ben Film3 1	PS	0.84	42-ben Film3 1	HDPE	0.5
42-ben Film3 2	PS	0.4	42-ben Film3 2	HDPE	0.97
42-ben Film3 3	PS	0.6	42-ben Film3 3	HDPE	1.1
average	PS	0.79	average	HDPE	0.89
standard deviation	PS	0.21	standard deviation	HDPE	0.31

Table S15. Experimental work of adhesion determined from probe tack measurements for PETE and PA-6 probes.

sample	probe	work of adhesion (mJ)	sample	probe	work of adhesion (mJ)
2-EH Film1 1	PETE	0.61	2-EH Film1 1	PA-6	0.47
2-EH Film1 2	PETE	0.68	2-EH Film1 2	PA-6	0.61
2-EH Film1 3	PETE	0.8	2-EH Film1 3	PA-6	0.46
2-EH Film2 1	PETE	0.69	2-EH Film2 1	PA-6	0.43
2-EH Film2 2	PETE	1.7	2-EH Film2 2	PA-6	0.68
2-EH Film2 3	PETE	0.36	2-EH Film2 3	PA-6	0.87
2-EH Film3 1	PETE	0.36	2-EH Film3 1	PA-6	0.81
2-EH Film3 2	PETE	1.1	2-EH Film3 2	PA-6	0.38
2-EH Film3 3	PETE	0.5	2-EH Film3 3	PA-6	0.37
average	PETE	0.76	average	PA-6	0.56
standard deviation	PETE	0.42	standard deviation	PA-6	0.19
42-ben Film1 1	PETE	0.69	42-ben Film1 1	PA-6	0.75
42-ben Film1 2	PETE	0.74	42-ben Film1 2	PA-6	0.58
42-ben Film1 3	PETE	0.48	42-ben Film1 3	PA-6	0.59
42-ben Film2 1	PETE	0.36	42-ben Film2 1	PA-6	0.39
42-ben Film2 2	PETE	0.73	42-ben Film2 2	PA-6	0.47
42-ben Film2 3	PETE	0.44	42-ben Film2 3	PA-6	1.1
42-ben Film3 1	PETE	0.83	42-ben Film3 1	PA-6	0.86
42-ben Film3 2	PETE	0.66	42-ben Film3 2	PA-6	0.23
42-ben Film3 3	PETE	0.83	42-ben Film3 3	PA-6	0.3
average	PETE	0.64	average	PA-6	0.59
standard deviation	PETE	0.17	standard deviation	PA-6	0.28

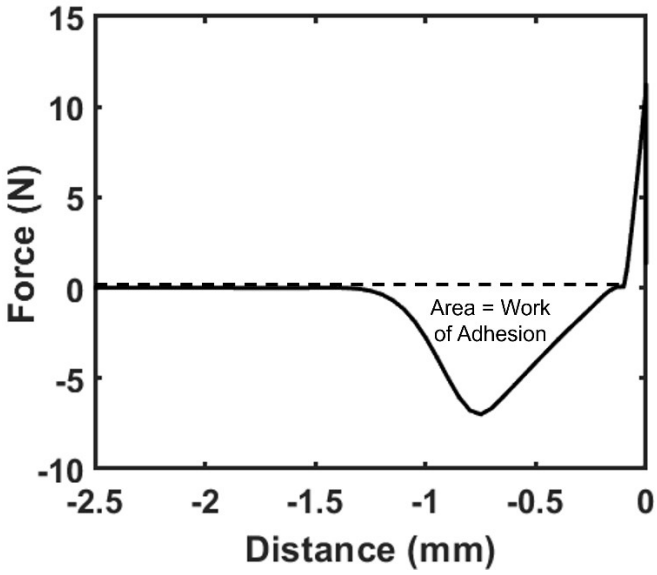

Figure S28. Representative force-displacement curve obtained from probe tack measurements during retraction (polymer = 2-EH; probe = stainless steel). Area under the dotted line represents work of adhesion. The work of adhesion is calculated by multiplying the force (N) by the distance (mm), where the unit N-mm is equivalent to mJ.

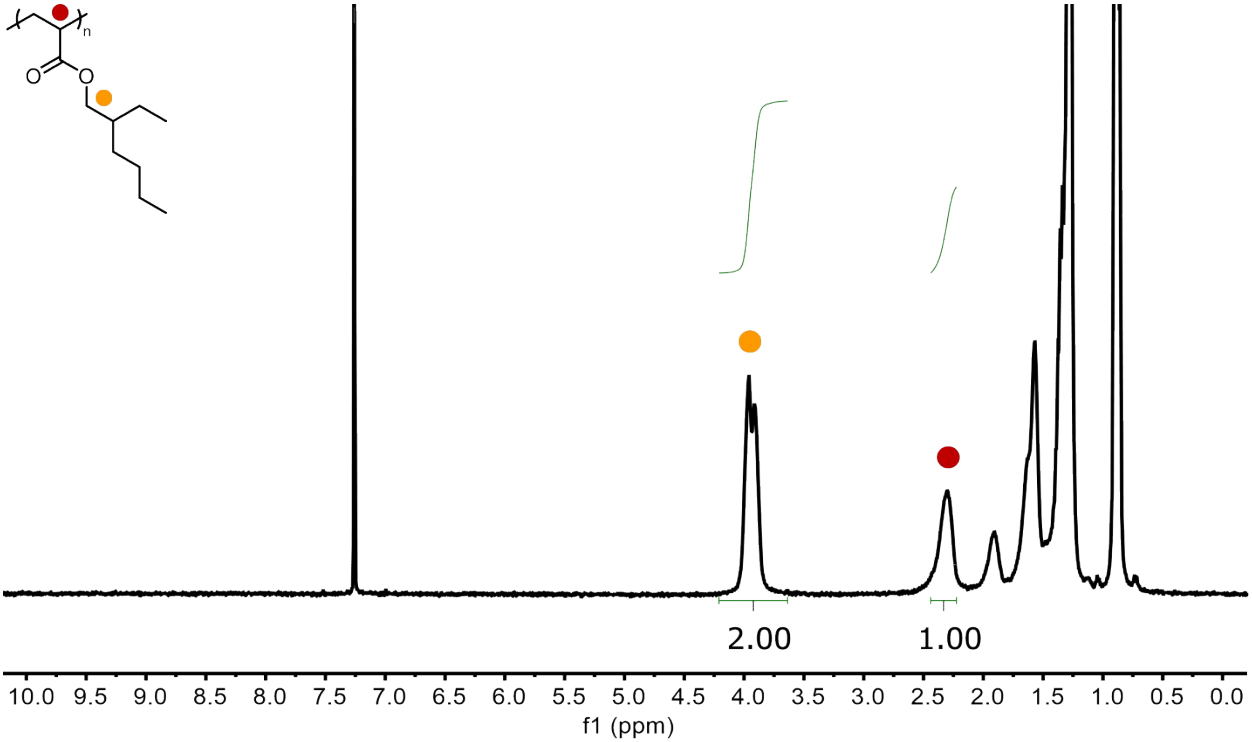

Figure S29. ^{1}H NMR spectra of 2-EH (400 MHz, $CDCl_3$)

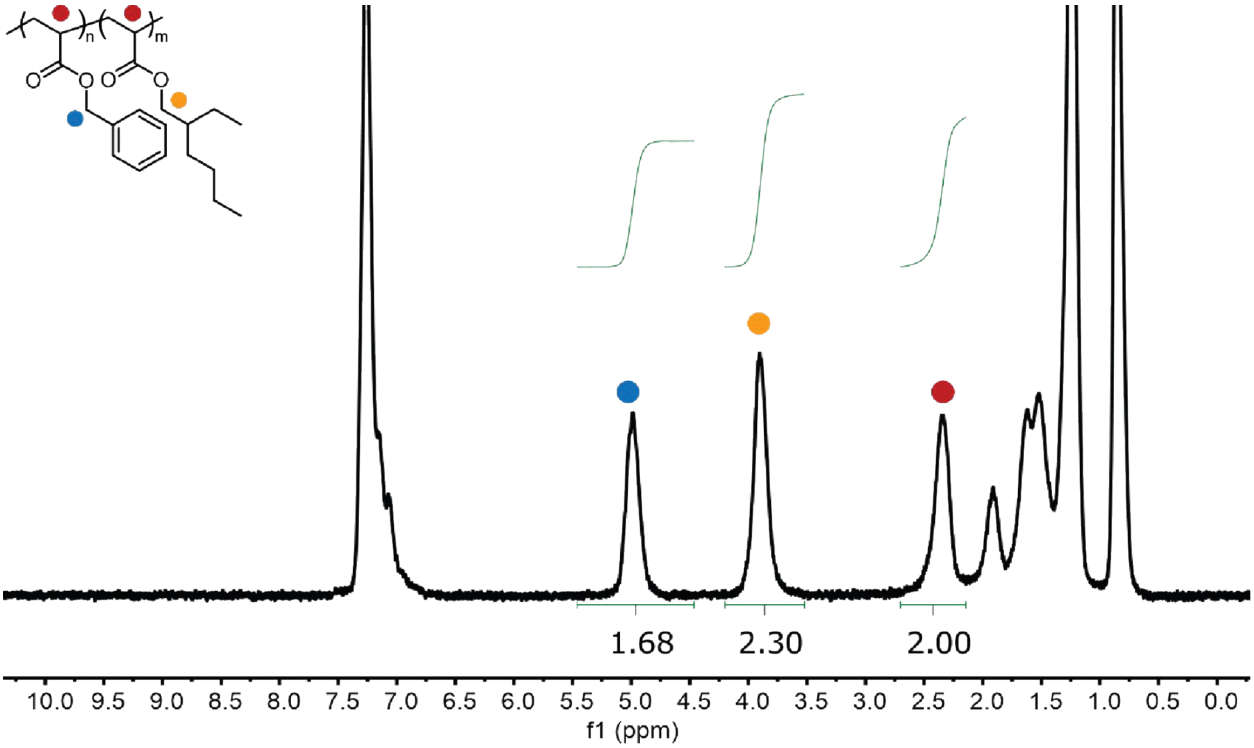

Figure S30. ^{1}H NMR spectra of 42-ben (400 MHz, $CDCl_3$)

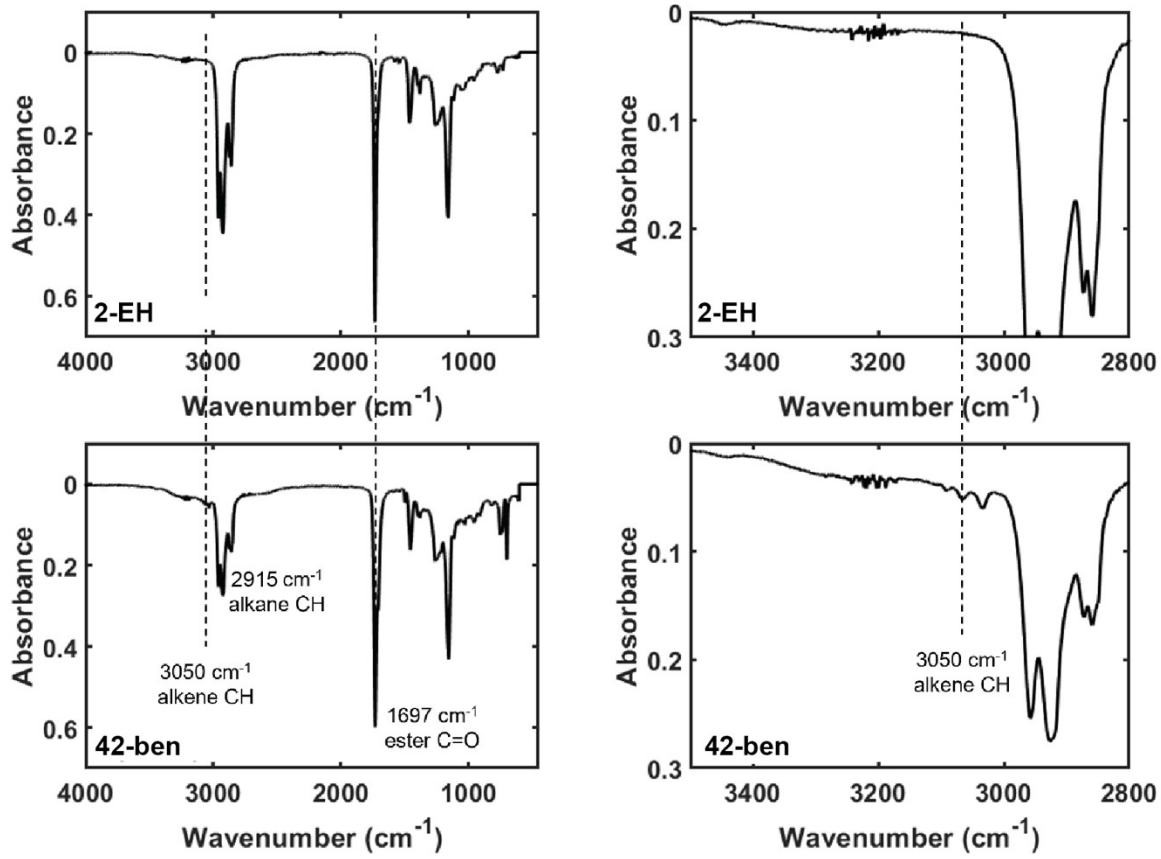

Figure S31. FT-IR spectra of 2-EH (top) and 42-ben (bottom).

18. References

1 P. Mark and L. Nilsson, *J. Phys. Chem. A*, 2001, **105**, 9954– 9960.
2 L. Martínez, R. Andrade, E. G. Birgin, and J. M. Martínez. *J. Comput. Chem*. 2009, **30**, 21572164.
3 W. M. Haynes, Ed., *CRC Handbook of Chemistry and Physics*, CRC Press, 2014.
4 George A. Jeffery; An introduction to hydrogen bonding, Oxford University Press, 1997
5 A. Kowalski, Z. Czech and Ł. Byczyński, *J. Coat. Technol. Res.*, 2013, **10**, 879–885.
6 M. Żenkiewicz, *Polym. Test.*, 2007, **26**, 14–19.